Supplement: Nearly optimal time-independent reversal of a spin chain

Aniruddha Bapat,[1,2,3,*] Eddie Schoute,[1,4,5,†] Alexey V. Gorshkov,[1,2,‡] and Andrew M. Childs[1,4,5,§]

[1] *Joint Center for Quantum Information and Computer Science, NIST/University of Maryland, College Park, Maryland 20742, USA*

[2] *Joint Quantum Institute, NIST/University of Maryland, College Park, Maryland 20742, USA*

[3] *Lawrence Berkeley National Laboratory, Berkeley, CA 94720, USA*

[4] *Department of Computer Science, University of Maryland, College Park, Maryland 20742, USA*

[5] *Institute for Advanced Computer Studies, University of Maryland, College Park, Maryland 20742, USA*

S1. TIME-DEPENDENT PROTOCOL FOR REVERSAL.

In this section, we give a simple analysis of the time-dependent protocol given in [S1, S2] using our methods. The strategy is to prove that this protocol satisfies Lemma 1 from the main text. Lemma 2 and Theorem 1 are then automatically satisfied. First, we re-introduce the protocol using our notation.

Protocol S1. Let $H_h := H(\mathbf{0}, \mathbf{1})$ and $H_J := H(\mathbf{1}, \mathbf{0})$, where $\mathbf{1} = (1, 1, \ldots, 1)$ and $\mathbf{0} = (0, 0, \ldots, 0)$. Explicitly,

$$H_h = \sum_{k=1}^{N} Z_k \,, \tag{S1}$$

$$H_J = X_1 + \sum_{k=1}^{N-1} X_k X_{k+1} + X_N \,. \tag{S2}$$

Apply $V := \left(e^{i\frac{\pi}{4}H_h} e^{i\frac{\pi}{4}H_J}\right)^{N+1}$ to the input state.

As in the main text, we extend the chain with two ancillary sites $\{0, N+1\}$ that constitute the edge E. The unitary V extends to an operator $\widetilde{V} := \mathbb{1}_E \otimes V$ on the extended chain. Then the following lemma holds.

* ani@lbl.gov

† eschoute@umd.edu

‡ gorshkov@umd.edu

§ amchilds@umd.edu

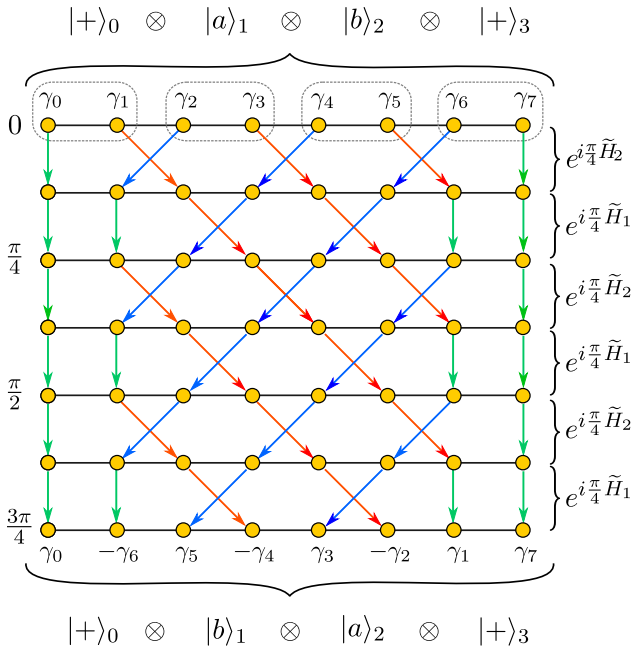

FIG. S1. Time-dependent reversal protocol for $N = 2$ (with two edge ancillas). For any bulk state $|ab\rangle_{12}$ (with edge state $|{+}{+}\rangle_E$), alternating $\pi/4$ evolutions under $\widetilde{H}_2$, $\widetilde{H}_1$ are applied a total of $2N + 2$ times. Each step braids neighboring Jordan-Wigner Majoranas as indicated by the arrows; the right-movers keep the same sign while the left-movers gain a minus sign. The edge Majoranas γ_0, γ_7 are unchanged (a crucial feature that ensures the correct parity phases), while the intermediate Majoranas undergo reversal of position with alternating sign. The final state in the bulk of the chain is $|ba\rangle_{12}$.

Lemma S2. *The operation $\widetilde{V}$ acts on the Majorana operators as*

$$\widetilde{V}\gamma_k\widetilde{V}^\dagger = \begin{cases} \gamma_k & \text{if } k = 0, 2N+3, \\ (-1)^{k-1}\gamma_{2N+3-k} & \text{otherwise.} \end{cases} \tag{S3}$$

Proof. We use Eq. (7) from the main text to write V as a product of alternating $\pi/4$-rotations under two Hamiltonians $\widetilde{H_J} = i\sum_{k=0}^{N}\gamma_{2k+1}\gamma_{2k+2}$ and $\widetilde{H_h} = i\sum_{k=1}^{N}\gamma_{2k}\gamma_{2k+1}$. Since $e^{-\pi/4\gamma_i\gamma_j}$ is a braiding unitary that maps $\gamma_i \mapsto \gamma_j, \gamma_j \mapsto -\gamma_i, \gamma_{k\neq i,j} \mapsto \gamma_k$, it follows that the operator $e^{i\frac{\pi}{4}\widetilde{H_h}}$ braids nearest-neighbor Majoranas along all odd edges of the chain (except the first and last edge), while $e^{i\frac{\pi}{4}\widetilde{H_J}}$ braids along the even edges. Therefore, alternating $\pi/4$ rotations under $\widetilde{H_J}$ and $\widetilde{H_h}$ implement an even-odd sort [S3] on the chain, as shown in Figure S1. Accounting for sign changes, the Majoranas map as follows: $\gamma_k \mapsto (-1)^{k+1}\gamma_{2N+3-k}$, while γ_0, γ_{2N+3} remain unchanged. □

S2. INFINITE FAMILY OF HAMILTONIANS FOR STATE REVERSAL.

Reference [S4] shows that there is an infinite family of XY Hamiltonians that generalize the protocol introduced in [S5]. In fact, Protocol 1 from the main text is also a special case of an infinite family of protocols parameterized by a single non-negative integer m, as given below.

Protocol S3. Let $m \in \mathbb{Z}_{\geq 0}$, and

$$J_k^{(m)} := \frac{\pi}{4}\sqrt{(2k+1+4m)\,(2N+1-2k+4m)} \tag{S4}$$

$$h_k^{(m)} := \pi\sqrt{k\,(N+1-k)} \tag{S5}$$

for all sites $k = 1, \ldots, N$. Let $H^{(m)} = H(\boldsymbol{J}^{(m)}, \boldsymbol{h}^{(m)})$. Apply $U^{(m)} := e^{-iH^{(m)}}$ to the input state.

The protocol modifies only the couplings $J_k^{(m)}$ as a function of m, while the field terms $h_k^{(m)} = h_k$ are invariant with m. Note that $U^{(0)} = U$, so Protocol 1 is indeed a special case of Protocol S3. For convenience, we have rescaled the coefficients so that the evolution time is 1. To prove the correctness of this family of protocols, write the Hamiltonian $H^{(m)}$ in terms of Majorana fermions obtained by Jordan-Wigner transformation on the spin chain (extended to edge sites $\{0, N+1\}$). We have

$$H^{(m)} = \frac{1}{2}\boldsymbol{\gamma} \cdot A^{(m)} \cdot \boldsymbol{\gamma}, \tag{S6}$$

where $\boldsymbol{\gamma} = \begin{bmatrix}\gamma_1 & \gamma_2 & \cdots & \gamma_{2N+2}\end{bmatrix}$ and $A^{(m)}$ is a $(2N+2) \times (2N+2)$ tridiagonal matrix with entries

$$A^{(m)} = i \begin{pmatrix} 0 & J_0^{(m)} & & & & \\ -J_0^{(m)} & 0 & h_1 & & & \\ & -h_1 & 0 & J_1^{(m)} & & \\ & & \ddots & \ddots & \ddots & \\ & & & -h_N & 0 & J_N^{(m)} \\ & & & & -J_N^{(m)} & 0 \end{pmatrix}. \tag{S7}$$

As before, the Heisenberg evolution of the Majoranas under $H^{(m)}$ is given by $\boldsymbol{\gamma}(t) = e^{2iA^{(m)}t}\boldsymbol{\gamma}(0)$. Lemma 1 (main text) shows that the operator $e^{2iA^{(0)}}$ implements reversal. Here we show that $e^{2iA^{(m)}} = e^{2iA^{(0)}}$ for all m, which implies that $U^{(m)}$ implements state reversal for all m. We state the following lemma (due to [S6, S7]) on the spectrum of $A^{(m)}$.

Lemma S4. *Let $A^{(m)}$ be as given in (S7), and $s_k \coloneqq \operatorname{sgn}(2N+3-2k)$. Then $A^{(m)}$ has spectrum*

$$E_k^{(m)} = \frac{\pi}{4}\left(2k - 2N - 3 + 4s_k m\right) \tag{S8}$$

for $k = 1, \ldots, 2N+2$. The corresponding eigenvectors v_k satisfy $v_{kj} = (-1)^{N+k-j+1/2} v_{k(2N+3-j)}$.

Proof. The first claim follows from [S6]. Via a transformation of the off-diagonals that preserves the spectrum, $A^{(m)}$ can be converted to a matrix $B(n,a)$ of Sylvester-Kac type

$$B(n,a) \coloneqq \frac{\pi}{4}\begin{pmatrix} 0 & 1+a & & & & & \\ n+a & 0 & 2 & & & & \\ & n-1 & 0 & 3+a & & & \\ & & \ddots & \ddots & \ddots & & \\ & & & 2 & 0 & n+a \\ & & & & 1+a & 0 \end{pmatrix}, \tag{S9}$$

for $n = 2N+1, a = 4m$. As shown in [S6], the eigenvalues of $B(n,a)$ are given by the formula $\lambda_{\pm,j} = \pm\frac{\pi}{4}|2j+1+a|$ for $j \in \{0, \ldots, n\}$, and the first claim follows.

For the second claim, we observe again that $A^{(m)}$ may be converted to a real, symmetric, tridiagonal matrix $C^{(m)}$ with positive off-diagonal entries via the similarity transformation $C^{(m)} \coloneqq DA^{(m)}D^{-1}$ where $D = \operatorname{diag}\left(i, i^2, \ldots, i^{2N+2}\right)$. Reference [S7] shows that the eigenvectors $u_k = Dv_k$ of $C^{(m)}$ (ordered by ascending eigenvalue) satisfy $u_{kj} = (-1)^{k-1} u_{k(2N+3-j)}$ for $k = 1, \ldots, 2N+2$. Correspondingly, the eigenvalues of $A^{(m)}$ satisfy $v_{kj} = (-1)^{k-1} i^{2N+3-2j} v_{k(2N+3-j)} = (-1)^{N+k-j+1/2} v_{k(2N+3-j)}$. □

Finally, we show that $e^{2iA^{(m)}}$ implements reversal.

Theorem S5. *For all $m \in \mathbb{Z}_{\geq 0}$, $A^{(m)}$ satisfies $\left[e^{2iA^{(m)}}\right]_{jl} = (-1)^{j-1}\delta_{j(2N+3-l)}$.*

Proof. Write

$$e^{2iA^{(m)}} = \sum_{k=1}^{2N+2} e^{2iE_k^{(m)}} v_k v_k^\dagger = \sum_{k=1}^{2N+2} (-1)^{k-N-3/2} v_k v_k^\dagger, \tag{S10}$$

where we dropped the trivial phase $2\pi i m s_k$. The matrix elements of $e^{iA^{(m)}}$ are

$$\left[e^{iA^{(m)}}\right]_{jl} = \sum_{k=1}^{2N+2} (-1)^{k-N-3/2} v_{kj} v_{kl}^* \tag{S11}$$

$$= \sum_{k=1}^{2N+2} (-1)^{2N+2-l} v_{kj} v_{k(2N+3-l)}^* \tag{S12}$$

$$= (-1)^{j-1}\delta_{j(2N+3-l)}\,, \tag{S13}$$

where in the second step we used Lemma S4 as $v^*_{kl} = (-1)^{l-k-N-1/2} v^*_{k(2N+3-l)}$. Therefore, $e^{2iA^{(m)}}$ maps $\gamma_k \mapsto (-1)^{k-1}\gamma_{2N+3-k}$, which implies that the protocol $U^{(m)}$ implements state reversal for all $m \in \mathbb{Z}_{\geq 0}$. □

When normalized so that all two-qubit terms are bounded by unity in spectral norm, $H^{(m)}$ implements state reversal in time $t_N^{(m)} = \frac{(N+1+4m)\pi}{4}$. Therefore, the time cost increases linearly in m and is minimal for Protocol 1 (main text) where $m = 0$. Next, observe that if we choose $4m \gg N$, the variation in coupling coefficients $J_k^{(m)}$ is small and on the order $\sim \frac{1}{8}\left(\frac{N+1}{2m}\right)^2$. Therefore, the parameter m quantifies a trade-off between reversal time and the non-uniformity of $J_k^{(m)}$. Setting $m = N+1$, for example, yields a variation in the couplings on the order of 3% for any N, and gives reversal in time $5N\pi/4$.

S3. ROBUSTNESS OF THE PROTOCOL.

Protocol 1 and its generalizations given in Section S2 are exact, i.e., any input state $|\psi\rangle$ maps perfectly to the output $\mathrm{R}|\psi\rangle$, assuming the interaction coefficients are implemented exactly as prescribed. However, inherent in experimental systems is noise, and the usefulness of a given state transfer protocol is determined not only by the time of operation and fidelity under perfect implementation, but also resilience to noise. Here, we model imperfect fabrication as a static noise term on every coefficient in the Hamiltonian. We compare our time-independent protocol with a swap-based protocol for reversal (odd-even sort) and a gate-based protocol [S1].

Stochastic noise can be modeled as a perturbation to the Hamiltonian coefficients. For the case of disorder, we draw a single noise term for every coefficient from the normal distribution $\mathcal{N}$. We assume that the noise is multiplicative, so that the noise strength scales proportional to the magnitude of the coefficient. The perturbed Hamiltonian H' for our time-independent protocol then looks like

$$H' = J'_0\sigma_x^1 + \sum_{k=1}^{N-1} J'_k\sigma_x^k\sigma_x^{k+1} + J'_N\sigma_x^N - \sum_{k=1}^{N} h'_k\sigma_z^k\,, \tag{S14}$$

where $J'_i = J_i \cdot (1+\delta J_i), h'_i = h_i \cdot (1+\delta h_i)$, where $\delta h_i \sim \mathcal{N}(\delta_h), \delta J_i \sim \mathcal{N}(\delta_J)$ for specified standard deviations $\delta_h, \delta_J \geq 0$. Evolution under this Hamiltonian gives a noisy reversal $\mathrm{R}' \coloneqq e^{-iH'_i t_N}$ that reduces to R when $\delta_h = \delta_J = 0$. For swap and gate-based protocols, we compute an equivalent Hamiltonian formulation and similarly add noise terms.

A natural and widely used metric for the distinguishability of outputs of two quantum channels is the completely bounded trace norm (or diamond norm) [S8]. The computation of the diamond norm can be efficiently expressed as the solution to a semidefinite program [S9], making it a somewhat non-trivial quantity to compute. We consider unitary noise models, where the diamond distance is equivalent to a simpler notion of distinguishability, the *spectral distance*

$$\Delta \coloneqq \|\mathrm{R}' - \mathrm{R}\|\,, \tag{S15}$$

where we take the spectral norm of the difference between perfect and noisy state reversals R and R′. In this case, the diamond distance is at most two times as large as the spectral distance [S10]. The distance Δ can be used to bound another common figure of merit, the *fidelity*

$$\mathrm{F}(\rho,\sigma) = \mathrm{Tr}\left(\sqrt{\sqrt{\rho}\sigma\sqrt{\rho}}\right), \tag{S16}$$

for output states ρ and σ evolved by a perfect and noisy reversal, respectively.

We will prove a bound on the minimum fidelity for completeness here but do not claim novelty of the result. First, we bound Δ by the minimum fidelity over pure states as follows:

$$\begin{aligned}
\Delta^2 &= \|(\mathrm{R}-\mathrm{R}')^\dagger(\mathrm{R}-\mathrm{R}')\| && \text{(S17)}\\
&= \max_{|\psi\rangle} |\langle\psi|(\mathrm{R}-\mathrm{R}')^\dagger(\mathrm{R}-\mathrm{R}')|\psi\rangle| && \text{(S18)}\\
&= \max_{|\psi\rangle} |\langle\psi|2\mathbb{1} - \mathrm{R}^\dagger\,\mathrm{R}' - \mathrm{R}'^\dagger\,\mathrm{R}|\psi\rangle| && \text{(S19)}\\
&= \max_{|\psi\rangle} |2 - 2\,\mathrm{Re}\,\langle\psi|\,\mathrm{R}^\dagger\,\mathrm{R}'|\psi\rangle| && \text{(S20)}\\
&= 2 - \min_{|\psi\rangle} 2\,\mathrm{Re}\,\langle\psi|\,\mathrm{R}^\dagger\,\mathrm{R}'|\psi\rangle && \text{(S21)}\\
&\geq 2 - 2\min_{|\psi\rangle} |\langle\psi|R^\dagger R'|\psi\rangle|\,, && \text{(S22)}
\end{aligned}$$

where we used the fact that for any unitary U, $\mathrm{Re}\,\langle\psi|U|\psi\rangle \leq 1$, and $\mathrm{Re}\,[z] \leq |z|$ for any $z \in \mathbb{C}$. Let $F_{\min}$ denote the worst-case fidelity over all input states. By the joint concavity of the fidelity [S11, Corollary 3.26], $F_{\min}$ is attained for a pure state, thus

$$F_{\min} = \min_{|\psi\rangle} \mathrm{F}(R'|\psi\rangle, R|\psi\rangle) = |\langle\psi|R^\dagger R'|\psi\rangle| \tag{S23}$$

since $\mathrm{F}(|\phi_1\rangle,|\phi_2\rangle) = |\langle\phi_2|\phi_1\rangle|$ for pure states $|\phi_1\rangle$ and $|\phi_2\rangle$. It then follows from (S22) that $F_{\min} \geq 1 - \frac{1}{2}\Delta^2$.

We estimate the spectral distance dependence on noise and system size in the three candidate protocols [S12]. For each protocol, we probe the distance as a function of similar on-site and coupling

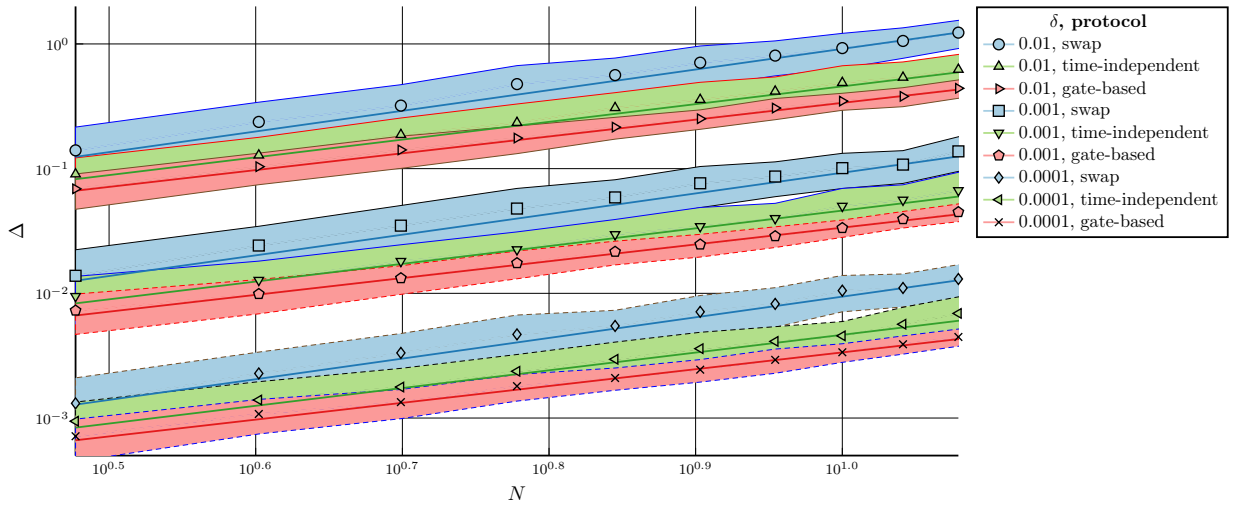

FIG. S2. Spectral distance mean values with standard deviation (shaded region) for different protocols under varying strengths of noise. We take 100 samples for each data point and use a linear fit for a power law $\Delta = \exp(N^a \delta^b)$ controlled on the protocol, i.e., fitting $\log \Delta = a \log N + b \log \delta + O(1)$, to find (standard error) $a \approx 1.66(0.012)$ and $b \approx 0.994(0.0028)$ for the SWAP-based protocol. The b coefficient changes insignificantly for time-independent and gate-based protocols but the a coefficient is reduced by 0.31(0.016) for gate-based and 0.23(0.016) for time-independent protocols, indicating more robust scaling of these protocols in system size, relative to a SWAP-based protocol.

disorder $\delta = \delta_h = \delta_J$, and increasing number of spins N. The spectral distance is computed by exact diagonalization, taking time exponential in N, and it is possible to probe system sizes up to $N = 14$ with the resources available. At these sizes, we can already see differences between the protocols, shown in Figure S2. At each error rate δ, the swap protocol has the worst performance, the time-independent protocol performs better, and the gate-based protocol has the best performance. We note that the gate-based and time-independent protocols perform within a standard deviation of one another, but the SWAP protocol is significantly noisier. For example, at a threshold of $\Delta \leq 0.03$, the swap can reverse only up to 4 sites, while the time-independent protocol can successfully reverse 8 sites. Therefore, the specialized protocols for reversal improve upon SWAP-based protocols not only in runtime but also in accuracy.

The relative performance of time-independent and gate-based protocols (including the SWAP protocol) may not be captured by our simulations. Since the time-independent protocol is static, it derives its error primarily from imperfect engineering of the coupling strengths and interactions with the environment. Gate-based protocols, however, require dynamical control, which could be

an additional source of noise. Since this noise source is likely to worsen the performance of discrete protocols, we cannot make a definite comparison between our protocol and gate-based protocols in our noise model.

[S1] R. Raussendorf, Quantum computation via translation-invariant operations on a chain of qubits, Phys. Rev. A **72**, 10.1103/physreva.72.052301 (2005).

[S2] J. Fitzsimons and J. Twamley, Globally controlled quantum wires for perfect qubit transport, mirroring, and computing, Phys. Rev. Lett. **97**, 10.1103/physrevlett.97.090502 (2006).

[S3] D. E. Knuth, The Art of Computer Programming: Sorting and Searching (Addison-Wesley Professional, 1998) Chap. Networks for Sorting, pp. 219–247, 2nd ed.

[S4] P. Karbach and J. Stolze, Spin chains as perfect quantum state mirrors, Phys. Rev. A **72**, 10.1103/physreva.72.030301 (2005).

[S5] C. Albanese, M. Christandl, N. Datta, and A. Ekert, Mirror inversion of quantum states in linear registers, Phys. Rev. Lett. **93**, 10.1103/physrevlett.93.230502 (2004).

[S6] R. Oste and J. Van der Jeugt, Tridiagonal test matrices for eigenvalue computations: Two-parameter extensions of the clement matrix, J. Comput. Appl. Math. **314**, 30 (2017).

[S7] O. H. Hald, Inverse eigenvalue problems for Jacobi matrices, Linear Algebra Appl. **14**, 63 (1976).

[S8] D. Aharonov, A. Kitaev, and N. Nisan, Quantum circuits with mixed states, in *Proceedings of the thirtieth annual ACM symposium on Theory of computing - STOC 98* (ACM Press, 1998).

[S9] J. Watrous, Semidefinite programs for completely bounded norms (2009), arXiv:0901.4709 [quant-ph].

[S10] A. Y. Kitaev, Quantum computations: algorithms and error correction, Russian Mathematical Surveys **52**, 1191 (1997).

[S11] J. Watrous, *The Theory of Quantum Information* (Cambridge University Press, 2018).

[S12] E. Schoute and A. Bapat, Noisy state reversal, `https://gitlab.umiacs.umd.edu/amchilds/noisy-state-reversal` (2021).